Heliyon 10 (2024) e28457

Contents lists available at ScienceDirect

Heliyon

journal homepage: www.cell.com/heliyon

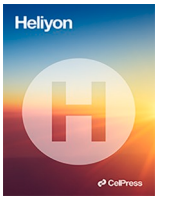

Research article

Enhanced efficacy of β-carotene loaded solid lipid nanoparticles optimized and developed via central composite design on breast cancer cell lines

Rajat Subhra Dutta [a,b,**], Gamal Osman Elhassan [c,*], Takhellambam Bidyapati Devi [d], Bedanta Bhattacharjee [a], Mohini Singh [b], Bani Kumar Jana [b], Supriya Sahu [a], Bhaskar Mazumder [b], Ram Kumar Sahu [e,***], Jiyauddin Khan [f]

[a] School of Pharmaceutical Sciences, Girijananda Chowdhury University-Tezpur Campus, 784501, Assam, India
[b] Department of Pharmaceutical Sciences, Dibrugarh University, Dibrugarh, 786004, Assam, India
[c] Department of Pharmaceutics, College of Pharmacy, Qassim University, Buraidah, 52571, Saudi Arabia
[d] Gautham College of Pharmacy, Sultanpalya, R.T Nagar, 560032, Bangalore, India
[e] Department of Pharmaceutical Sciences, Hemvati Nandan Bahuguna Garhwal University (A Central University), Chauras Campus, Tehri Garhwal, Uttarakhand, India
[f] School of Pharmacy, Management and Science University, 40100, Shah Alam, Selangor, Malaysia

ARTICLE INFO

Keywords:
β-carotene
Anti-cancer
Solid lipid nanoparticles
Drug development
Bioavailability
In-vitro
Poloxamer-407

ABSTRACT

β-carotene is obtained from both plants and animals and has been the subject of intense research because of its provitamin-A, antioxidant, and anticancer effects. Its limited absorption and oxidative degradation significantly reduce its antitumor efficacy when taken orally. In our study, we utilize a central composite design to develop "bio-safe and highly bio-compatible" solid lipid nanoparticles (SLNs) by using only the combination of palmitic acid and poloxamer-407, a block co-polymer as a surfactant. The current research aim to develop and characterize SLNs loaded with β-carotene to improve their bioavailability and therapeutic efficacy. In addition, the improved cytotoxicity of solid lipid nanoparticles loaded with β-carotene was screened *in-vitro* in human breast cancer cell lines (MCF-7). The nanoparticles exhibits good stability, as indicated by their mean zeta potential of -26.3 ± 1.3 mV. The particles demonstrated high drug loading and entrapment capabilities. The fabricated nanoparticle's prolonged release potential was shown by the *in-vitro* release kinetics, which showed a first-order release pattern that adhered to the Higuchi model and showed a slow, linear, and steady release over 48 h. Moreover, a diffusion-type release mechanism was used to liberate β-carotene from the nanoparticles. For six months, the nanoparticles also showed a notable degree of physical stability. Lastly, using the MTT assay, the anti-cancer properties of β-carotene-loaded solid lipid nanoparticles were compared with intact β-carotene on MCF-7 cell lines. The cytotoxicity tests have shown that the encapsulation of β-carotene in the lipid bilayers of the optimized formulation does not interfere with the anti-cancer activity of the drug. When compared to standard β-carotene, β-carotene loaded SLNs

* Corresponding author.
** Corresponding author. School of Pharmaceutical Sciences, Girijananda Chowdhury University-Tezpur Campus, 784501, Assam, India
*** Corresponding author.
E-mail addresses: rajatsubhra7@gmail.com (R.S. Dutta), go.osman@qu.edu.sa (G.O. Elhassan), ramsahu79@gmail.com, ramkumar.sahu@hnbgu.ac.in (R.K. Sahu).

https://doi.org/10.1016/j.heliyon.2024.e28457
Received 13 December 2023; Received in revised form 16 March 2024; Accepted 19 March 2024
Available online 25 March 2024

showed enhanced anticancer efficacy and it is a plausible therapeutic candidate for enhancing the solubility of water-insoluble and degradation-sensitive biotherapeutics like β-carotene.

1. Introduction

Breast cancer (BC) accounts for more than 10% of new cancer cases in women, making it the most common disease in this population [1–3]. It is currently the second leading cause of cancer-related deaths in the female population [4]. In 2023, 609,820 cancer deaths and 1,958,310 new cancer cases are expected worldwide. Consequently, the likelihood of developing BC is increased by a familial predisposition to BC [5]. For the year 2023, 609,820 cancer deaths and 1,958,310 new cancer cases are expected worldwide. Consequently, the probability of developing BC is increased by a family predisposition to BC [6]. The necessity for BC treatment and the high patient death rate drives technical advancements in terms of accessibility, affordability, and side effect safety [6,7]. The three systemic approaches employed in the treatment of BC include chemotherapeutic, site-specific, and hormonal-targeted therapy [8]. Current treatment methods for BC involve the use of anthracyclines derivatives *viz* epirubicin or doxorubicin, methotrexate, 5-fluorouracil, and cyclophosphamide [8–10]. The upregulated growth-promoting protein HER2/neu requires site-specific treatment in about 17% of BC patients. The first medication to be authorized is a monoclonal antibody called trastuzumab, which specifically targets the HER2 protein [8]. Tamoxifen is the cornerstone of hormonal therapy for the majority of premenopausal women with hormonal receptor-positive malignancies. It is reported to have a number of adverse effects (AEs) associated with chemotherapeutic drugs such as alopecia, neutropenia, anemia, nausea, neuropathic pain, lymphedema, and vomiting [8,11,12].

This emphasises the need for phytomedicine in the treatment of BC to overcome the side effects associated with chemotherapeutic agents [13]. Carotenoids are naturally tetraterpenoids pigments that have antioxidant characteristics as well as anticancer activities. About 95% of the carotenoids in the bloodstream are β-carotene, α-carotene, β-cryptoxanthin, lycopene, and lutein [14]. The Food and Drug Administration (FDA) has classified β-carotene as generally regarded as safe (GRAS) and approved its consumption as a vitamin additive in neonates and adult diets. β-Carotene has remarkable anticancer effects through a variety of molecular processes involving transcription factors, intercellular interaction at gap junctions, singlet (O_2^-) oxygen scavenging, suppression of peroxy radicals, inhibition of cell cycle progression and expansion, induction of apoptosis, suppression of metastasis and angiogenesis [14]. The risk of BC has been inversely correlated with β-carotene. In this context, examining the connection between β-carotene and BC is vital before developing or designing any formulation. Peraita-Costa et al. conducted a study in which they analyzed prominent databases such as PubMed and EMBASE for the period from 2014 to 2020 [14,15]. The survey included only epidemiologic studies on the association between β-carotene and BC. The included studies provide evidence of a correlation between β-carotene and BC risk, suggesting that β-carotene can be consumed reduce BC risk [16,17]. Studies on humans, both prospective and retrospective, clearly show that β-carotene offers protection against various types of cancer. It can protect against a range of malignancies of the colon, stomach, ovary, cervix, breast, and other cancers. Carotenoids are vulnerable to oxidative modifications because of their unsaturated nature. β-carotene appears to be the protective element having increased rate of apoptosis and stopping the cell cycle at distinct periods, thereby decreases cell proliferation which highlights the β-carotene as an interesting target for pharmacological intervention with BC [14]. Several human BC cell lines experienced growth inhibition by β-carotene, leading to apoptosis and cell-cycle arrest [18]. It has been revealed that β-carotene is the cause of the reduction of cyclin A, a crucial regulator of the advancement of the cell cycle. According to *in-vitro* research, this carotenoid may have chemotherapeutic properties against BC [19]. The cellular cycle of these BC cells is disrupted, and they are unable to regulate how fast they proliferate. One of the rate-limiting events of the cell cycle, the G1 phase of cell division, is severely impaired under BC conditions [19].

The solubility of β-carotene in aqueous solutions is limited due to its strong hydrophobic nature. It is also extremely susceptible to oxidation when exposed to light, oxygen, or heat because of its high degree of instauration [20]. Recent advances in nanotechnology may provide useful ways to overcome the drawbacks of β-carotene. The majority of research on nano-carotenoids has been about using nanotechnology to make nano-sized carriers for carotenoids, characterising and testing how stable they are, and looking into their release, bioavailability, and pharmacological activity in vitro [20,21]. In the last decade, much work has been done to improve the bioavailability of β-carotene through nano-formulation approaches. However, there are many drawbacks associated with conventional nanoparticle-based systems like poor bioavailability, low entrapment efficacy, and poor shelf life. In their research, Soukoulis et al. explored how assembling carotenoids into a nanoemulsion may improve their chemical stability and bioavailability. Nanoemulsions might be able to help make β-carotene more bioavailable, but they have some problems that need to be thought about. For example, they need a lot of surfactant and cosurfactant, they do not last very long, they can not dissolve compounds with high melting points, and they are very harmful to living things [22]. Studies conducted by Dos Santos et al. pointed out that polymeric nanoparticles can be used for the encapsulation of carotenoids and represent a cost-effective nano-drug delivery system [23]. Some polymeric nanocarriers with biodegradable polymers may cause uncontrollable release and leakage of the drug and could show a few drawbacks associated with irritation after administration through subcutaneous, intramuscular, and intravenous routes and very poor shelf life [24,25]. Rehman et al. stated in their recent study that carotenoid-based nanoliposomes demonstrated a reduced size and polydispersity index, but there are major drawbacks associated with nanoliposomes like low entrapment efficiency, limited susceptibility to gastrointestinal enzymes, inadequate solubility, low consistency, problems controlling liposome size, and short half-life [26]. To address the above-mentioned limitation of conventional nanoparticles, we have presented a proposal for the further development of a drug delivery system centered on solid lipid nanoparticles (SLNs).

SLNs presents various advantages over conventional drug delivery systems which includes long term physical stability as evidenced

from the stability study data reported in various publications with different drugs. SLNs provide enhanced bioavailability, lower cyotoxicity due to its biocompatible nature and also the drug release can be modulated as rate controlled or sustained release over longer period of time.

Delivery methods based on solid lipids aims to make the carotenoids transported in more soluble and micelle-like form. Also, the formulation's solid lipid content helps to stimulate pancreatic and bile secretion, which makes it easier for lipids to break down and carotenoids to be absorbed [14]. The final structure of the nanocarrier and the selection of appropriate formulation ingredients can control the bioavailability of carotenoids. In addition, the systems need to be as compact as feasible and resistant to gastrointestinal (GI) conditions, such as low pH and GI enzymes. Recently, some work has been done on the development of SLNs using β-carotene. One of the common features of these studies is the use of more than one co-surfactant alongside the solid lipid to stabilize the nanoparticles. Preparation of SLNs involves the incorporation of various grades of surfactants and co-surfactants like cationic, anionic, non-ionic, and alcoholic grades [14]. However, due to toxicity concerns, it is advisable to limit the use of too many combinations of surfactants and co-surfactants. For instance, there are recent reports that polysorbate-80, a non-ionic surfactant, is not an inert substance, similar to certain other surfactants, and it has been connected to certain systemic, injection, and infusion-site adverse events (ISAEs) and hypersensitivity systemic responses (HSRs) [27]. Similarly, there are various reports of toxicity studies of ionic surfactants [28].

β-carotene has certain advantages over other naturally occurring substances due to its effectiveness as provitamin-A having antioxidant as well as anticancer effects as reported in various literatures. On the other hand, encapsulating β-carotene in SLNs would result in greater bioavailability, excellent stability, higher drug loading as well as prolonged release. Moreover, with the advancement of nanotechnology this β-carotene loaded SLNs would provide greater cell permeability which will aid to target the cancer cell due to their nano-size range. Thus, β-carotene SLNs would be more effective than conventional dosage form [14].

The benefits of multiple colloidal carriers of its class are combined with the avoidance of their disadvantages by SLNs. This effort is distinct from other nanoparticle based studies that has been reported in literature so far, as it employs solid lipid-based delivery strategies designed to enhance the solubility of carotenoids with many advantages over other conventional nanoparticles like, improved stability of pharmaceuticals, higher drug content, excellent biocompatibility and more affordable. The restricted availability of safe polymers with regulatory approval and their high cost have prevented nanoparticles from being widely used in clinical treatment. These are a new class of submicron-sized lipid emulsions in which a solid lipid has been used in place of the liquid lipid (oil). Small size, vast surface area, high drug loading, and phase interaction at interfaces are some of the distinctive qualities that make SLNs appealing due to their potential to enhance the delivery of water insoluble therapeutics [14].

Hence in our study, we aim to design a "bio-safe and highly bio-compatible" SLNs by using only the combination of palmitic acid (PA) and poloxamer-407, a block co-polymer as a surfactant. In a 2008-based study on the safety assessment of various grades of poloxamers, it was reported that poloxamer-407 is one of the safest and biocompatible cosurfactants to use with no serious reports of adverse effects [28]. Looking at this we have aimed to enhance the physicochemical stability of β-carotene by loading it in SLNs stabilized with PA and poloxamer-407. To safeguard the β-carotene that was encapsulated, a solid shell is created by PA crystals. PA core was combined with poloxamer-407, a non-ionic surfactant, to create a miscible surfactant shell. The surfactant decreases surface contacts between the individual SLNs to offer steric stabilization, which increases the stability of SLNs adding to their colloidal and steric stability [29].

2. Materials and methods

2.1. Materials

Poloxamer-407, palmitic acid, ethanol, ether, and chloroform were obtained from Merck, Mumbai. Pure β-carotene powder and MTT [3-(4,5-dimethylthiazol-2-yl)-2,5-diphenyltetrazolium bromide] was procured from the supplier Sigma Aldrich, Bangalore. The MCF-7 breast cancer cell lines were acquired from the National Centre for Cell Sciences (NCCS) in Pune, India.

2.2. Physicochemical characterization of drug

The physicochemical characterization of the drug was performed by.

2.2.1. Physical observations

The color and powder forms of the drug were observed and identified as per the standard.

2.2.2. Determination of Melting point of β-carotene

To identify the β-carotene, the melting point of the compound was determined using a melting point apparatus (Remi). The melting point of the sample tested and verified with the reported melting point.

2.2.3. Solubility

At 25 °C, the solubility of β-carotene was observed in different solvents, including water, ether, 95% ethanol, and chloroform [30].

2.2.4. UV–visible spectrometric analysis

The UV–visible spectrum of β-carotene was recorded by scanning its solution in dichloromethane (0.001% w/v) at the wavelength between 300 nm and 700 nm and the absorption maxima was recorded [31].

2.3. β-carotene -excipients compatibility studies

2.3.1. Fourier transform infrared spectroscopy (FT-IR) study

An IR spectrometer was used to record the FT-IR band. A study on the compatibility between drugs and excipients was conducted using FT-IR spectroscopy with the NICOLET iS10 (Omnic software). The band was acquired within the wave number range of 600–4000 cm^{-1}, with a resolution of 4 cm^{-1}. Each band represents a mean of 32 scans. FT-IR studies were performed for β-carotene, PA, poloxamer-407, physical mixture of drugs, and prepared β-carotene loaded SLNs [32].

2.3.2. Differential scanning calorimetry (DSC) thermogram analysis

DSC (PERKIN ELMER DSC 6000) was utilized to perform DSC experiments on the samples. A dry nitrogen purge of 20 mL/min was applied to the DSC cell. Precisely measured specimens (3–5 mg) were subjected to a temperature range of 15–450 °C in a conventional aluminum pan, with a heating rate of 20 °C/min [31].

2.4. Preparation of β-carotene SLNs

The solvent diffusion methodology was used to prepare the SLNs, with a few changes. Several formulations were prepared in different combinations of palmitic acid and poloxamer-407 utilizing the data obtained from central composite design (Table 2). In brief, palmitic acid (ranging from 0.659104 to 2.3409 mg/mL for different formulations) was dissolved in ethanol at 70 °C to create a lipid phase and β-carotene (20% w/w of the palmitic acid concentration) was added further to that lipid phase. The aqueous phase was prepared by dissolving poloxamer-407 at different concentrations (ranging from 0.159104 to 1.8409 % for different formulations) in deionized water and the system temperature was maintained at 45 °C. Subsequently, the lipid phase containing β-carotene was promptly added to the aqueous phase containing poloxamer-407. The mixture was then mechanically homogenized using a high-speed homogenizer (Ultra Turrax T10 Basic, IKA) at a speed of 7000 rpm and the temperature was maintained at 45 ± 2 °C. The dispersion was homogenized for 10 min, followed by cooling to ambient temperature, resulting in the formation of the SLNs [33]. The volume of ethanol and water was adjusted at a ratio of 1:10 (v/v). Drug-free blank preparations were also developed using the same procedure. The formulation was further lyophilized according to the protocol used by Osanlou et al. with minor changes. The SLNs dispersion (50 mL) was first frozen under −40 °C in a deep freezer, and then the samples were dried using a lyophilizer (freeze-drier). The drying time was controlled for up to 72 h to get the SLNs powder. The lyophilized powder was kept at −40 °C in amber containers covered with aluminum foil and parafilm, shielded from moisture and light [33]. The weight ratio of the analyzed weight of SLNs to the theoretical weight of SLNs was used to characterize the recovery of SLNs, and it was computed using equation (1):

$$\%\ Recovery = \frac{(Analyzed\ weight\ of\ SLNs)}{(Theoretical\ weight\ of\ SLNs)}\ x\ 100 \tag{1}$$

2.5. Optimization of the prepared SLNs using central composite design (CCD)

2.5.1. Experimental design using response surface methodology (RSM)

In this study, RSM was utilized to investigate the influence of three specific parameters, namely lipid concentration (A), surfactant concentration (B), and stirring speed (C), on particle size (E) and β-carotene entrapment efficiency (F). This experiment was designed using a quadratic model and central composite design (CCD). A total of 20 runs were created, comprising 6 central, 8 factorial, and 6 axial points. Table 1 presents a subset of variables together with their coded values.

The real levels of the distinct factors were coded using equation (2):

$$M = M_A\text{-}\ M_C/\Delta M \tag{2}$$

where coded and real levels of distinct factors are denoted by M and M_A, accordingly. A step change is represented by ΔM, while the actual value at the central point is shown by M_C. From the preceding equation, the particular formulas were created to code the actual values of each distinct factor.

equations (3)–(5) provided below pertain to the quantification of lipid concentration (A), surfactant concentration (B), and stirring speed (C):

$$M_1 = (LC\text{-}1.5)/0.5 \tag{3}$$

Table 1
Illustration of Distinct factors and their corresponding coding levels for β-carotene for β-carotene SLNs.

Distinct Factors	Representation	Coded Levels				
		-α	−1	0	+1	+α
Lipid concentration (mg/mL)	A	0.6591	1.00	1.50	2.00	2.34
Surfactant concentration (%)	B	0.1591	0.50	1.0000	1.50	1.84
Stirring speed (RPM)	C	5659.10	6000.00	7000.00	6500.00	7340.90

Table 2
Particle size and β-carotene EE values with distinct factors obtained using the CCD.

Run	Distinct Factors			Response Values	
	Lipid Concentration (mg/ml)	Surfactant Concentration (%)	Stirring Speed (rpm)	Particle Size (nm)	β-carotene EE (%)
1	1.5	1.8409	6500	114.7	46.9
2	1	0.5	7000	97.5	56.33
3	1.5	1	6500	103.4	66.77
4	1.5	1	6500	101.2	64.52
5	2	1.5	6000	125.7	60.2
6	2	0.5	6000	135.3	64.3
7	1	1.5	6000	102.5	49.5
8	1.5	1	6500	94.1	62.5
9	0.659104	1	6500	84.4	53.5
10	1	0.5	6000	114.2	57.55
11	1.5	1	7340.9	80.03	62.3
12	1.5	0.159104	6500	125.7	55.5
13	2	1.5	7000	98.3	59.5
14	2	0.5	7000	113.9	61.3
15	1.5	1	6500	100.8	65.5
16	1.5	1	6500	100.5	64.5
17	1.5	1	5659.1	124.9	62.5
18	1	1.5	7000	80.3	53.4
19	1.5	1	6500	98.1	61.5
20	2.3409	1	6500	110.9	65.4

$$M_2 = (SC\text{-}1)/0.5 \tag{4}$$

$$M_3 = (SS\text{-}6500)/500 \tag{5}$$

Where LC, SC, and SS represent lipid concentration, surfactant concentration, and stirring speed, respectively.

The Design Expert software (version 7.0) was used to carry out the statistical analysis. The best-fitting numerical model was determined by a comparative analysis of several statistical parameters of quadratic designs, such as the lack-of-fit, adjusted multiple correlation coefficient (adjusted R^2), predicted multiple correlation coefficient (predicted R^2), and coefficient of variation (CV). The significance of the variation was determined by applying the analysis of variance (ANOVA), which led to the calculation of the F-value at probabilities of 0.05 or 0.01. The 3D response plots of the model fits were created using Design Expert software to better understand the effect of the selected factor on the responses.

2.6. Analysis of prepared SLNs

2.6.1. Estimation of particle size and zeta potential

The size of the particles and zeta potential of the developed SLN dispersions were measured with a Litesizer 500 from Anton Paar utilizing Kalliope software at a temperature of 25 °C. This was accomplished by measuring the dynamic light scattering (DLS). To minimize the influence of multiple scattering, lyophilized samples of powder were mixed with deionized water to the proper concentration before being measured. The electrophoretic mobility was measured to estimate the zeta potential, and a field strength of 20V cm^{-1} was provided. The samples were diluted in deionized water before testing [34].

2.6.2. Percentage of drug entrapment efficiency (DEE)

DEE (%) was calculated using the protocols described by Nazemiyeh et al. and Triplett et al. UV–visible spectroscopy was employed to determine DEE (%)of SLNs. The original SLNs dispersion was spun in a centrifuge for 45 min at 14500 rpm to quantify the DEE. Both the separated supernatant and the pellet were collected. The supernatant collected was used for the determination of free drugs or unentrapped drugs in the SLNs. The UV measurement of the SLNs preparations was performed using the previously developed calibration graph. A wavelength of 461 nm was used for all absorbance observations [35,36]. The DEE in the SLNs was calculated from equation (6):

$$\text{DEE}\ (\%) = \frac{(\text{total amount of drug taken}) - (\text{un} - \text{entrap drug})}{concentrationofdruginitiallytaken} x100 \tag{6}$$

2.6.3. Examination of samples using scanning electron microscopy (SEM)

Using SEM, the SLNs surface topology was assessed. A dispersion of aqueous nanoparticles was meticulously spread on a surface and later subjected to drying under a stream of nitrogen gas. Subsequently, a fast auto-coater was used to vacuum-coat the sample with a gold coating. Using a scanning electron microscope, the electron microscopic images were captured (Zeiss Sigma VP) [36].

2.7. In-vitro release studies

Nazemiyeh et al. reported that the dialysis methodology was used for carrying out the overall *in-vitro* release of β-carotene SLNs. In the dialysis membrane bag, the SLNs suspension (MW limit 12–14 kDa) was charged. The bag was then placed within a type-II apparatus, which included a glass container holding 50 mL of pH 7.4 phosphate buffer. The medium was constantly swirled at 37 ± 0.5 °C for the duration of the investigation at a speed of 100 rpm and during the predetermined intervals. 4 mL of the sample was removed, and 4 mL of the new medium was added to the glass container at the designated interval. To find out how much of the drugs were present, a UV spectrophotometer with a wavelength of 461 nm was used. For up to 48 h, the trial was conducted [35]. After fitting the release values with a zero-order, first-order, Higuchi and Korsmeyer-Peppas model, the mechanism of drug release from the formulated SLNs was determined [37].

2.8. Physical stability studies

Based on the results of studying the different phases and formulation factors, the best β-carotene SLNs were chosen to be tested for stability further. To determine how stable the prepared SLNs were, the samples were stored in a refrigerator set at 4 °C for a period of six months. The samples were observed for particle aggregation, DEE%, and DL% and compared with the fresh ones [35].

2.9. Effectiveness of optimized β-carotene SLNs using in-vitro cell line investigation

2.9.1. Cell lines and culture medium

MCF-7 BC cell lines were grown to confluence in Dulbecco's Modified Eagle's Medium (DMEM) in a humidified 5% CO_2 atmosphere at 37 °C. The medium was supplemented with amphotericin B (5 g/mL), streptomycin (100 g/mL), and penicillin (100 IU/mL). In addition, the media contained 10% foetal bovine serum (FBS). Stock cultures were maintained in 25 cm^2 cell culture flasks and 96 microtitre plates were used for each experiment (Tarsons India Pvt. Ltd., India) [38].

2.9.2. Estimation of in-vitro cell cytotoxicity

The MTT assay was performed on MCF-7 BC cell lines to assess whether or not the SLNs loaded with β-carotene have an enhanced cytotoxic effect compared to pure β-carotene The cell population was seeded in 96-well plates at a density of 5 x 10^3 cells per well. After exposure to nanoparticles and pure β-carotene at different concentrations (5, 10, 20, 40, 60, 80, 100, and 200 μg mL^{-1}), the cells, which were 70–80% confluent, were incubated for 24 h. After adding 20 μL of MTT solution (5 mg/mL) to each well, the plate was returned to the cell incubator for a further 4 h of incubation. After the medium was removed, 150 mL of dimethyl sulfoxide (DMSO) was added to the cells. Before the measurement with a Spectramax M2 Microplate Reader (Molecular Diagnostic, Inc.) at 570 nm, the plate was gently shaken for 15 min to break up the cell formazan crystals that were forming. The relative viability of the cells was determined by establishing a baseline value of 100% as a control using wells with untreated cells. The results are expressed as average values (±SEM) of three replicates [39].

3. Results and discussions

3.1. Physicochemical characterization studies

3.1.1. Physical observation, melting point, and solubility determination

The β-carotene appeared to be dark orange in color and had a melting point in the range of 180–185 °C, which corresponds to the reported melting of β-carotene. The β-carotene was shown to be immiscible in water and soluble in chloroform, moderately soluble in ether, and sparingly soluble in 95% ethanol which meets the standard specifications [31].

3.1.2. UV–visible spectrometric analysis

The absorption maximum of the UV–visible spectrum of β-carotene was found to be 461 nm, which corresponds to the 461 nm

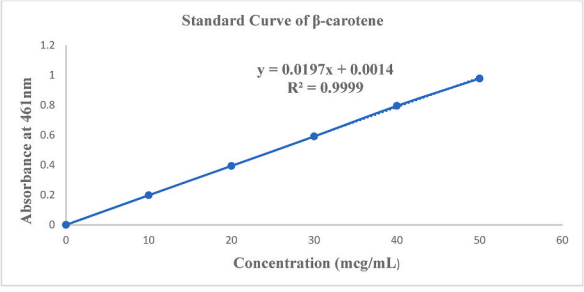

Fig. 1. Standard curve of β-carotene.

absorption maximum of the standard. A standard curve was developed using various concentrations of β-carotene in the range of 10–50 μg/mL as represented in Fig. 1 [31].

3.2. Drug-excipients compatibility studies

3.2.1. FT-IR spectroscopic screening

FT-IR band of β-carotene, poloxamer-407, palmitic acid (PA), physical mixture of drug, and prepared β-carotene loaded SLNs are depicted in Fig. 2 respectively. The IR-band of the pure β-carotene show principal bands at 2930 cm^{-1} (-C-H stretching), 1716 cm^{-1} (-C═O stretching), 1455 cm^{-1} (-C-H- bending vibration from methylene of carotenoids), 1366 cm^{-1} (β-ionone ring of β-carotene due to symmetrical bonding), and 966 cm^{-1} (C–H out of plane/C═C bending) (Fig. 2 A) [32]. The characteristics band of poloxamer-407 are observed at 2882 cm^{-1} (-C-H stretching), 1343 cm^{-1} (in-plane O–H bending), and 1100 cm^{-1} (-C-O stretching) (Fig. 2 B). The characteristics band of PA is shown at 2918 cm^{-1} (-C-H stretching), 2850 cm^{-1} (-C-H stretching), 1695 cm^{-1} (-C-C stretching), and 1464 cm^{-1} (-*O*-H bending) (Fig. 2C) [32]. The physical mixture of drugs shows characteristics bands at 2916 cm^{-1} (-C-H stretching), 1698 cm^{-1} (-C-C stretching), 1471 cm^{-1} (-*O*-H bending), 1342 cm^{-1}(in-plane O–H bend), 1100 cm^{-1} (-C-O stretching), and 963 cm^{-1} (C–H out of plane/C═C bending) which indicates that there is no interaction between β-carotene and the physical mixture (Fig. 2 D) [32]. However, these major bands of the β-carotene are found to have disappeared in the IR-band of formulated β-carotene loaded SLNs which indicates that the drug is entrapped inside the lipid core (Fig. 2 E) [32]. The disappearance of a new peak in the β-carotene loaded SLN spectrum when contrasted to its blank suggests that β-carotene has just dissolved in the lipid matrix and has not undergone any chemical interactions with the additional nanoparticle components [32].

3.2.2. DSC thermogram analysis

DSC analysis was carried out for β-carotene, PA, poloxamer-407, and β-carotene loaded SLNs using PerkinElmer DSC 6000 at the rate of 10 °C per minute. A distinct endothermic peak can be seen in the DSC thermograms of β-carotene (Fig. 3 A), PA (Fig. 3 B), and poloxamer-407 (Fig. 3C) at 183 °C, 69 °C, and 70 °C, respectively. On the other hand, the β-carotene loaded SLNs display a complete disappearance of the endothermic peak of β-carotene *i.e.* at 183 °C but it shows the characteristic peak at 69 °C (Fig. 3 D). The disappearance of the characteristic peak of the pure drug may be since the drug is molecularly dispersed in the lipid matrix and demonstrating the drug's interaction with the lipids as well as the development of van der Waals or hydrogen bond interactions. It indicates that the drug encapsulated in the lipid core [31]. Furthermore, studies suggest that the amorphous form of β-carotene explains its better solubility compared to crystalline drugs.

3.3. Preparation of β-carotene loaded SLNs

The β-carotene SLNs were prepared successfully and the % recovery of the SLNs was found to be 70.61 ± 1.60%. However, the prepared formulation has to be optimized based on the particle size and DEE and characterized to obtain stable SLNs. Therefore, the formulations were optimized using the CCD model (Fig. 4 A and B) [33].

3.4. CCD optimization of β-carotene loaded SLNs

3.4.1. Fitting the model

The number of distinct factors can be optimized by using the mathematical, theoretical, and statistical approach of response surface methodology (RSM). Table 2 shows the effect of the distinct factors on the particle size (E) and β-carotene EE (F). Utilizing experimental data, quadratic equation coefficients were calculated to forecast response variable values [40]. The regression equations for individual response variables that were obtained using RSM are shown in equations (7) and (8):

$$\text{Particlesize} = +99.64 + 9.03\text{A-}5.32\text{B-}11.95\text{C} + 0.4625\text{AB-}1.24\text{AC-}1.44\text{BC-}0.4528\text{A}^2 + 7.52\text{B}^2 + 1.25\text{C}^2 \quad (7)$$

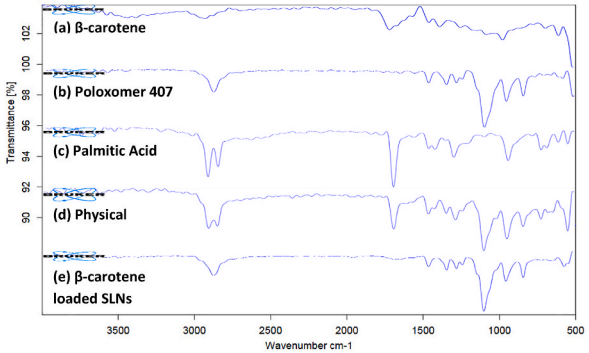

Fig. 2. FT-IR band of (a) β-carotene, (b) PA, (c) Poloxamer-407, (d) Physical mixture of β-carotene and excipients, and (e) β-carotene loaded SLNs.

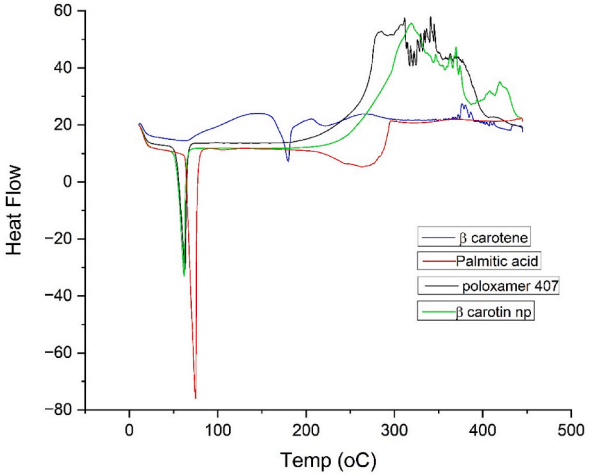

Fig. 3. Superimposed DSC thermogram (a) β-carotene, (b) Poloxamer-407, (c) PA, and (d) β-carotene loaded SLNs.

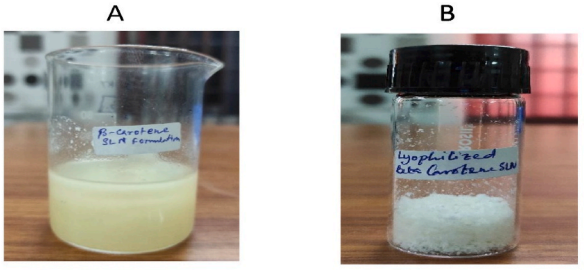

Fig. 4. Visual appearance of (A) solid lipid nanodispersion of optimized formulations and (B) lyophilized powder.

$$\beta\text{-carotene entrapment efficiency} = +64.20 + 3.55A\text{-}2.30B\text{-}0.0993C + 0.6350AB\text{-}0.7975AC + 0.9275BC\text{-}1.58A^2\text{-}4.50B^2\text{-}0.5419C^2 \quad (8)$$

The findings of statistical analysis (ANOVA) showed that a quadratic polynomial model accurately represented the experimental data for particle size (E) and β-carotene EE (F), with regression coefficient (R^2) values of 0.9711 and 0.9644 respectively (Table 3).

All variables exhibit a lack of fit to a simple error that is not statistically significant ($p < 0.05$), which indicates the statistical correctness of our model. A model that fits the data more accurately is indicated by an R^2 value that is closer to unity. Conversely, lower R^2 values mean that the response variables were insufficient to account for the behavior deviation. The study indicates that a quadratic polynomial model may well represent the effects of lipid concentration (A), surfactant concentration (B), and stirring speed (C) on response variables, as evidenced by the closeness to unity R^2 value. The analysis of variance (ANOVA) method was utilized to ascertain the degree of significance value for the coefficients of the quadratic polynomial equation. It is evident that all factors have a significant impact on the response variable. This is indicated by a larger F-value and a smaller P-value [41].

Table 3
Coefficients of regression for SLNs containing β-carotene.

Regression Coefficient	Particle Size (nm)	β-carotene drug EE (%)
Intercept	99.64	64.20
A- Lipid Concentration	9.03	3.55
B- Surfactant Concentration	−5.32	−2.30
C- Stirring Speed	−11.95	−0.0993
AB	0.4625	0.6350
AC	1.24	−0.7975
BC	1.44	0.9275
A^2	0.4528	−1.58
B^2	7.52	−4.50
C^2	1.25	−0.5419
R^2	0.9711	0.9644

3.4.2. Influence of distinct factors on response parameters

β-carotene loaded SLNs were effectively developed with varying degrees of distinct factors. The influence of distinct factors on particle size and β-carotene EE are summarized in Table 2. The values of the regression coefficients for SLNs containing β-carotene are illustrated in Table 3.

3.4.2.1. Particle size. The concentration of surfactant was shown to have a significant influence on particle size at a quadratic ($p < 0.001$), and interaction level ($p < 0.05$) with stirring speed in β-carotene loaded SLNs. The concentration of lipid was shown to have a significant influence on particle size at a quadratic ($p < 0.0001$) and interaction level ($p < 0.05$) with stirring speed in β-carotene loaded SLNs. The stirring speed was shown to have a significant influence on particle size at a quadratic ($p < 0.0001$) and interaction level ($p < 0.05$) with surfactant in β-carotene loaded SLNs. Fig. 5 (A, B, and C) depicts how the concentration of lipids, the speed of the stirring, and the amount of surfactant all have an effect on the particle size [42].

The influence of lipid concentration and surfactant concentration on the β-carotene loaded SLNs particle size appears in Fig. 5 (A). As seen in Fig. 5(A)–a higher concentration of the lipid phase resulted in larger particles. This phenomenon can be attributed to an increase in the viscosity of the lipid-solvent diffusion phase, which leads to a decrease in the diffusion rate of the solute molecules [43]. Moreover, an increase in the concentration of the lipid phase leads to an increase in the amount of interactions and aggregations of the SLNs [44]. As a result, there is an ideal limit for the lipid concentration. The particle size decreases with increasing lipid concentration at low lipid phase concentrations and eventually reaches a minimum limit. When a surfactant is present, it lowers the interfacial tension between water and the solvent. This makes the surface area of the solvent-lipid particles spread out bigger, which then causes very small particles to form [45]. Furthermore, insufficient surfactant concentration can cause dispersions of nanostructured lipid carriers (NLC) dispersions to become unstable. As the surfactant concentration increases, the surface tension decreases, causing the particles to become smaller until they reach their smallest possible size. Fig. 5 (B) illustrates how the particle size of β-carotene SLNs is affected by the concentration of lipids as well as the speed of stirring *i.e.* greater particle size with increasing stirring speed at increasing lipid concentration [46]. Fig. 5 (C) illustrates how the surfactant concentration and stirring speed have an impact on the particle size of -carotene SLNs. These two factors have a quadratic influence on particle size. The particle size of SLNs reduced with increasing stirring speed at greater surfactant concentrations. This decreasing pattern was seen due to a decrease in interfacial tension as surfactant concentration increased. The particle size increased with increasing agitation speed at decreasing surfactant concentration [47].

3.4.2.2. β-carotene entrapment efficiency. The concentration of surfactant had a significant effect on the entrapment efficiency of the beta-carotene loaded SLNs. This effect was observed at a quadratic ($p < 0.001$) and interaction level ($p < 0.05$), with p-values indicating high statistical significance. As a result, the encapsulation efficiency of β-carotene in SLNs was dependent on the surfactant concentration. The concentration of lipid also had a significant effect on the entrapment efficiency of the beta-carotene loaded SLNs. This effect was observed at a quadratic ($p < 0.0001$), and interaction level ($p < 0.05$), with p-values indicating high statistical significance. The stirring speed did not have significant effect on drug EE ($0.1<p$).

Fig. 6 (A, B, and C) illustrates the effect that the concentration of lipids, the concentration of surfactants, and the stirring speed have on the amount of β-carotene EE. The effect that the concentration of lipids and surfactants has on the amount of β-carotene EE from SLNs is illustrated in Fig. 6 (A) β-carotene EE increased with increasing lipid concentration. β-carotene EE decreased with lower surfactant concentrations [40]. Fig. 6 (B) depicts the influence of stirring speed and lipid concentration on the β-carotene EE in SLNs. At higher lipid concentrations, β-carotene EE increases dramatically with increasing stirring [40]. Fig. 6 (C) shows the influence of stirring speed and surfactant concentration on the β-carotene EE in SLNs. The surfactant concentrations have a linear effect, but the stirring speed has a quadratic effect on the β-carotene EE. At lower surfactant concentrations, β-carotene EE decreases drastically with

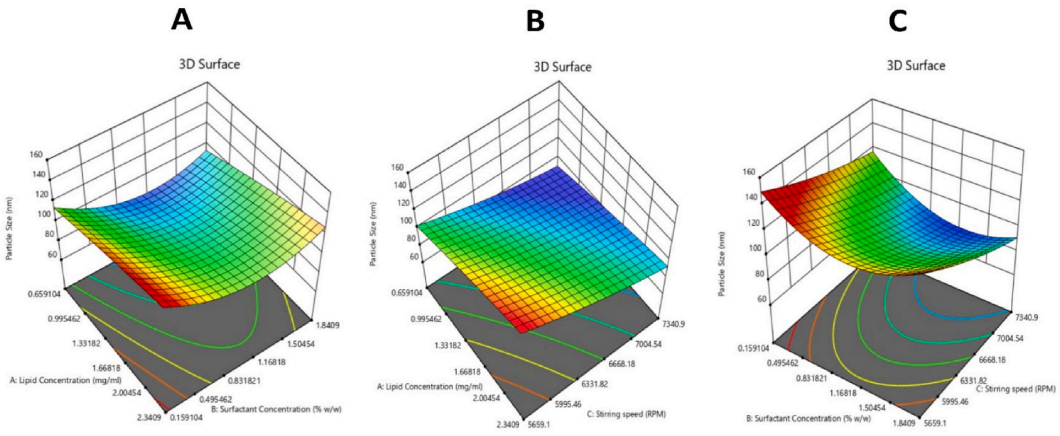

Fig. 5. Optimization of the 3D graphic surface of (A) particle size (nm) v/s lipid concentration (mg/mL) and surfactant concentration (%), (B) particle size (nm) v/s lipid concentration (mg/mL) and stirring speed (RPM), and (C) particle size (nm) v/s surfactant concentration (%) and stirring speed (RPM).

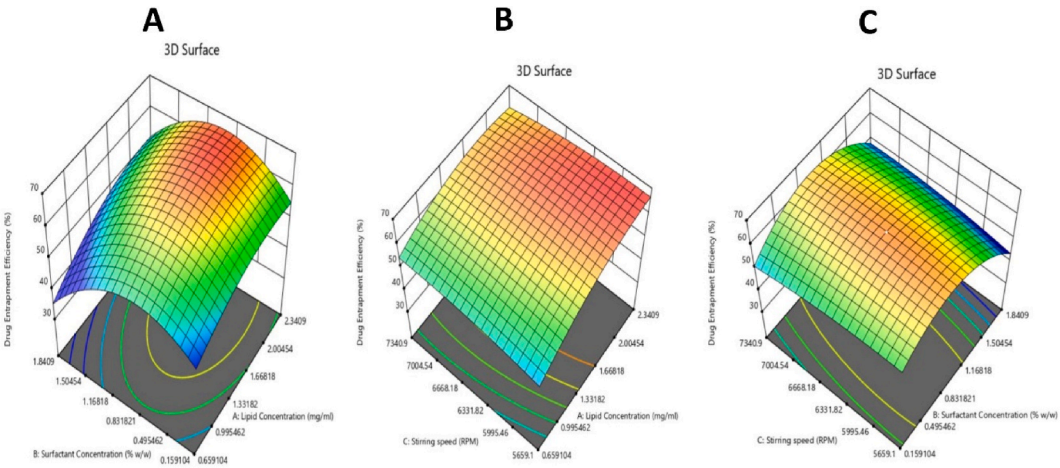

Fig. 6. Optimization of the 3D graphic surface of (A) drug EE v/s surfactant concentration (%) and lipid concentration (mg/mL), (B) drug EE v/s stirring speed (RPM) and lipid concentration (mg/mL), and (C) drug EE v/s stirring speed (RPM), and surfactant concentration (%).

increasing stirring speed due to the formation of tiny particles that are not protected by surfactant molecules [40].

3.4.3. Optimization of distinct factors

Reaction surface plots were created using Design Expert software to show how stirring speed, surfactant concentration, and lipid concentration affected response variables. Two different factors were varied within the experimental ranges to create these graphs, with the third variable remaining at a central point. Numerical optimization was then performed using Design Expert software with the desirability module. In order to achieve the highest DEE and smaller particle size of β-carotene, the optimization of β-carotene loaded SLNs was aimed at minimizing lipid concentration, surfactant concentration, and stirring speed. Twenty different solutions were identified, each with a varying degree of different factors. The optimal condition was determined by selecting the option with the highest desired value. A lipid concentration of 1.55 mg/mL, a surfactant concentration of 0.80%, and an agitation speed of 7000 rpm were the best settings for making β-carotene-loaded SLNs. At ideal preparation settings, the response values were 93.78 nm particle size and 63.58% β-carotene DEE (Table 4) [40].

3.5. Characterization studies of prepared SLNs

3.5.1. Estimation of particle Size and PDI

In the present study, the Z-average described the mean particle size of the test samples. The PDI, which assesses the homogeneity and distribution of particle sizes, is the second crucial collection of data obtained from the DLS evaluations. These are, in fact, some of the most crucial variables that affect how the nanoscale carrier interacts with its target site. Moreover, PDI can show the uniformity of the particles across the particle sample, as well as the aggregation of nanoparticle. The PDI value can actually be between 0 and 1. Colloidal particles with a PDI value of less than 0.1 are assumed to be monodisperse particles, while values greater than 0.1 indicate polydisperse particle size distributions. Moreover, values of 0.2 and below are usually considered acceptable in practice for lipid-based nanoparticle materials. In the system-generated standard report of DLS analysis, a major peak was found with 101.11 nm constituting 96.09% of nanoparticles, though there were two minor peaks present with 14.23 nm and 0.71 nm constituting 2.46% and 1.45% nanoparticles, respectively. The SLNs size distribution was varied in the range having a z-average of 111.78 nm with a PDI of 24.0% (found in the system-generated standard report of analyzed SLN sample using Kalliope software on Litesizer 500, Anton Paar) or 0.24 when converted into decimal points (Fig. 7). Hence, the particle size is within the nano scale range as desired and the PDI points towards an acceptable monodispersity of the particles [34]. It shows the consistency and homogeneity of the size distribution of the SLNs.

Table 4
Data of experimental, and predicted value at optimized condition.

Optimal Conditions Coded Levels Actual Levels		
Lipid Concentration (mg/ml)	+0.10	1.55
Surfactant Concentration (%)	−0.40	0.80
Stirring Speed (RPM)	+1.00	7000
Response	**Predicted Values**	**Experimental Values**
Particle Size (nm)	93.78	111.78
Drug Entrapment Efficiency (%)	63.58	66.46

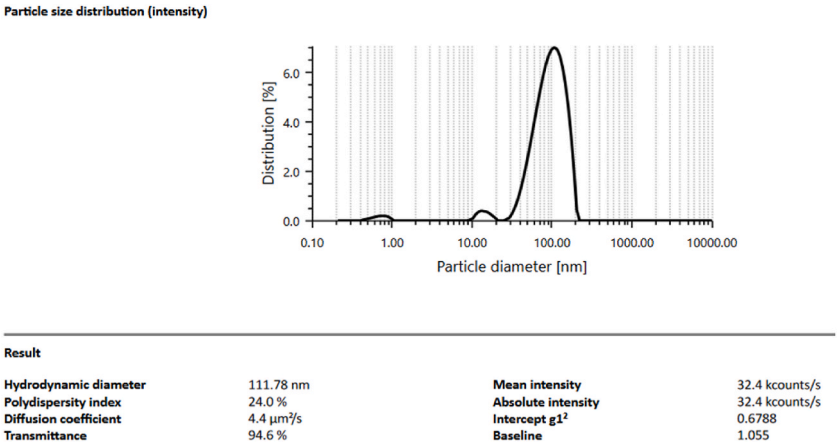

Fig. 7. β-carotene-loaded SLNs' average particle size.

3.5.2. Zeta potential

In this investigation, the zeta potential of the SLNs dispersions loaded with β-carotene was ascertained immediately after preparation. Predictions concerning the stability of the dispersion of colloidal particles are made possible by the measurement of the zeta potential. Fig. 8 illustrates the zeta potential of the developed SLNs formulations. The results showed that the optimized formulation has a mean zeta potential value of -26.3 ± 1.3 mV, which means that it possesses more flocculation for repulsion and more of the average amount of the usual threshold levels for attraction. The higher negative zeta potential of the β-carotene that is generated is explained by the existence of complexes, which also preserve the dynamic stability of β-carotene in aqueous environments. The distribution map of the zeta potential (Fig. 8) has shown a few numerous peaks, which correspond to distinct charged components in the SLNs sample. As a result, the produced β-carotene showed exceptional stability, as evidenced by the enhanced formulation's high zeta potential, small vesicular size, and restricted monodisperse size distribution [34].

3.5.3. SEM analysis

SEM is a direct method for the physical characterization of nanoparticles. The SLN formulation loaded with β-carotene exhibited a spherical shape with a smooth surface. No obvious aggregation of the SLNs could be seen on the SEM image (Fig. 9). The spherical and smooth shape of the particles is often preferred for uptake by lymphoid tissue cells, as spherical particles can be taken up more easily than uneven and misshapen particles [36].

3.6. In-vitro drug release

In general, all SLN formulations have shown a number of beneficial properties, including a minimal burst effect and a uniform release rate. Moreover, drug molecules form a strong bond with the lipid matrix in the SLNs, which may improve the drug release profile. The mechanism of drug release is critical for each formulation. Degradation, erosion, or diffusion are the mechanisms responsible for drug release from SLNs. The composition and nature of the lipid determine the drug's release mechanism from the SLN matrix. Drugs in SLN systems are either surface or matrix-embedded, and they can exhibit dual release or both immediate and prolonged release. These nanocarriers have the ability to control drug release over a significantly longer period of time and solubilize

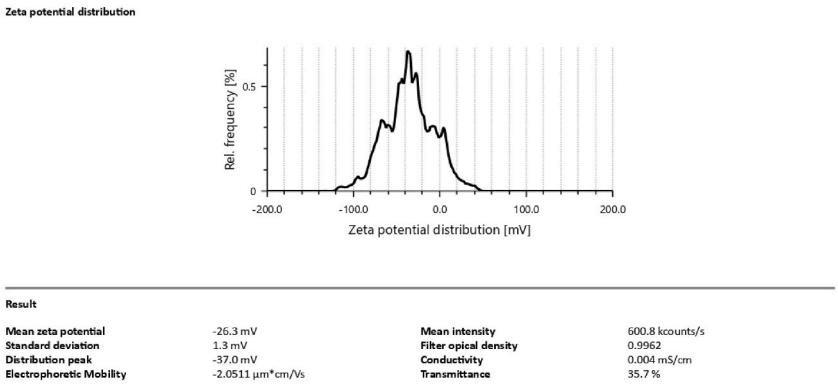

Fig. 8. Graph of zeta potential of the β-carotene-loaded SLN.

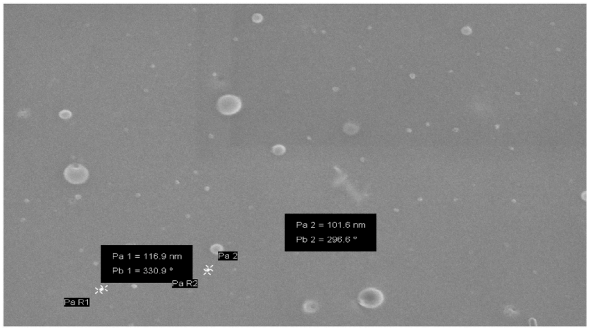

Fig. 9. SEM analysis of β-carotene-loaded SLN.

poorly water-soluble therapeutic molecules. The lipid structure of SLNs helps make chylomicrons and improves drug absorption into the lymphatic system, which keeps the liver from breaking down the drug. Usually, SLNs show a first initial burst release for 1 h, then a comparatively slower and more controlled release that lasts for 48 h. The initial explosive release is due to the adsorption of β-carotene on the surface of the particles or its exclusive presence in the first layer of the SLNs. During the second phase of sustained release, the β-carotene molecules that are integrated move across the SLN lipid matrix. It was also shown that the low water solubility profile of quercetin was enhanced by the amphiphilic nature of cholesterol and phospholipids. The *in-vitro* release study of optimized β-carotene-loaded SLNs was evaluated using a USP type-II apparatus utilizing a dialysis membrane bag with a molecular weight cutoff between 12 and 14 kDa. The SLNs showed significantly prolonged drug release which indicates that they can provide the desired sustained release over a prolonged time. A 48-h release assay was performed. It was found that 62.5% β-carotene had been released from the SLNs suspension after 12 h. However, the SLNs show a slow-release pattern maintaining a constant and linear release up to 48 h, during which a total of 89.7% β-carotene was released. The release profile of β-carotene has been shown to have a more favorable release pattern. Therefore, β-carotene encapsulated in a lipid matrix successfully improves bioavailability [35].

3.7. Drug release kinetics study

A number of different kinetic models were used to show how the drug released from the SLN preparation and how much was released over the course of the test. To determine the drug release mechanism of the SLNs loaded with β-carotene, the release data were fitted into zero-order, first-order, Korsmeyer-Peppas, and Higuchi kinetic models (Fig. 10 A, B, C, and D). The SLNs showed a release of up to 62.5% β-carotene in 12 h and a total of 89.7% β-carotene was released in 48 h. The slopes of the applicable plots were used to compute the release constant and the regression coefficient (R^2). The R^2 values found in zero-order, first-order, Korsmeyer-Peppas, and Higuchi kinetic models were 0.825, 0.965, 0.922, and 0.931 respectively. The SLNs loaded β-carotene were best fitted by first-order release kinetics where the R^2 value is 0.965 followed by the Higuchi equation with an R^2 value of 0.931. The kinetics of drug release shows that it is concentration-dependent. The Korsmeyer-Peppas equation demonstrated good linearity and the release exponent $n = 1.001$ for comprehending the process of drug release from SLN. A value of *n* greater than 0.89 indicates the super case II transport mechanism of diffusion justifying the developed SLNs formulation as a sustained release [37].

3.8. Physical stability

The stability of the SLNs was tested by storing the dispersion at 4 °C for six months. After six months, the drug EE and drug loading were calculated and compared with that of fresh dispersion. The entrapment efficiency of the fresh dispersion was 66.77% and had decreased to 58.93% after six months. The drug loading was also reduced from 11.13% to 9.82% (Table 5). This study suggests that the SLN was stable during the storage period [35].

3.9. In-vitro cell line study

Using the MTT assay and the MCF-7 BC cell line, it was possible to compare the potential cytotoxic effects of standard and carotene-loaded SLNs. The result showed that the cytotoxicity was significantly increased in the SLNs ($IC_{50} = 14.89 \pm 0.02$) as compared to the standard β-carotene ($IC_{50} = 182.6 \pm 0.25$). The activity was more pronounced in β-carotene loaded SLNs as illustrated in Table 6. The better effectiveness of β-carotene SLNs against tumour cells may be due in part to the higher drug accumulation inside cells caused by nanoparticle absorption (Figs. 11 and 12). The β-carotene-loaded SLNs formulation showed great cytotoxicity in BC cell lines. It also had a lot of potential for targeting the breast by parenteral administration and had unique physical properties that made it very stable and effective at entrapment. The β-carotene loaded SLN formulation possesses greater permeation and retention phenomena leading to higher tumor diffusivity and passive targeting capabilities.

The bioavailability of β-carotene was enhanced by the lymphatic uptake of β-carotene by incorporation into SLNs. Therefore, our proposed method either alone or in conjunction with other strategies such as immunotherapy, osmotic pressure and mitochondrial targeting is a promising alternative for the prophylaxis and therapy of BC. β-carotene is considered an ideal SLN preparation as it

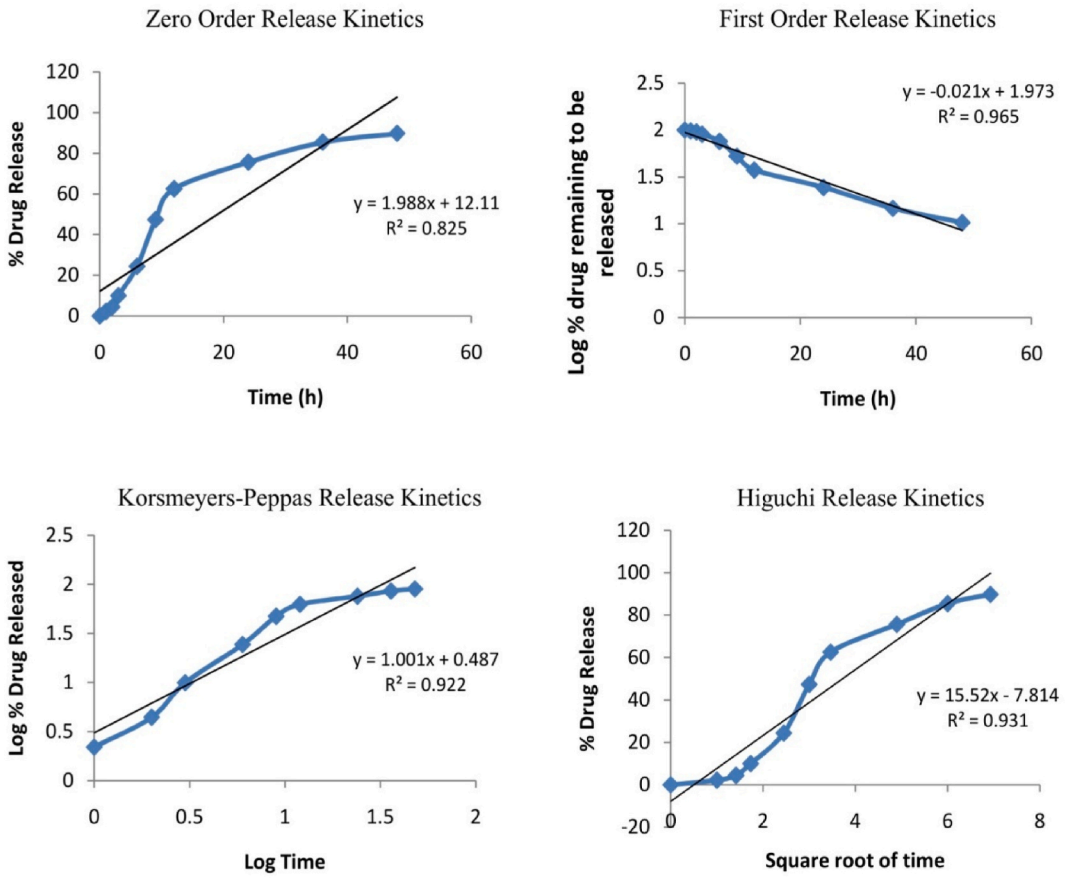

Fig. 10. Kinetic Model parameters of β-carotene loaded SLN of (A) Zero order release kinetics, (B) First order release kinetics, (C) Korsmeyers-Peppas release kinetics, and (D) Higuchi release kinetics.

Table 5
Physical stability study.

Drug entrapment efficiency (%)			Drug loading capacity (%)		
Fresh dispersion	After 1 month	After 6 months	Fresh dispersion	After 1 month	After 6 months
66.77 ± 1.03	60.38 ± 0.79	58.93 ± 1.37	11.13 ± 1.26	10.06 ± 0.54	9.82 ± 2.18

Table 6
The cell cytotoxicity concentration of MCF-7 BC cells lines against β-carotene loaded SLNs.

Concentration (μg/ml)	Pure β-carotene	IC_{50}	β-carotene loaded SLNs	IC_{50}
5	5.19 ± 0.02	182.6 ± 0.25	42.905 ± 0.07	14.89 ± 0.02
10	17.58 ± 0.13		69.17 ± 0.08	
20	26.10 ± 0.09		98.35 ± 0.03	
40	34.15 ± 0.01		144.08 ± 0.02	
60	35.99 ± 0.01		180.98 ± 0.07	
80	38.58 ± 0.01		224.70 ± 0.05	
100	40.17 ± 0.005		294.87 ± 0.01	
200	49.54 ± 0.072		367.96 ± 0.01	

combines all the beneficial properties, including strong physical characteristics, homogeneous drug release, a high level of cytotoxicity in cancer cell lines, and the absence of potentially harmful or unfavorable components. To fully characterize the pharmacological safety profile and explain the reported anticancer efficacy, further studies are required to evaluate the *in-vivo* efficacy and stability of our proposed SLNs approach [38].

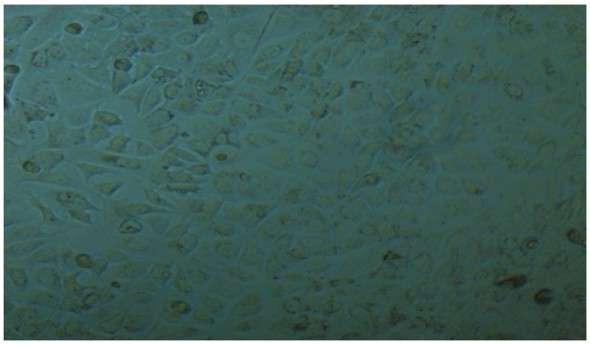

Fig. 11. Treated MCF-7 BC cell line with standard β-carotene.

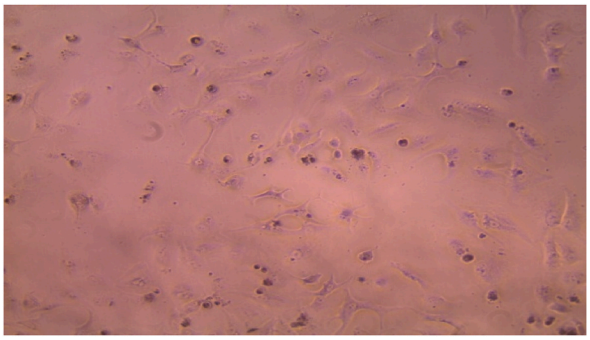

Fig. 12. Treated MCF-7 BC cell line with β-carotene-loaded SLNs.

4. Conclusion

β-carotene a poorly water-soluble active ingredient, was incorporated into an SLNs by solvent diffusion technique. The entire process was optimized using design expert software and a Central Composite was chosen as the model. PA was used as lipid and poloxamer-407 as a surfactant and stabilizer. The FTIR analysis which is a part of the pre-formulation studies, revealed that β-carotene is compatible with the other excipients and the absence of the major bands for β-carotene in the FTIR of the formulation indicated that the drug is encapsulated. Whereas, the DSC study indicated a molecular dispersion of β-carotene in the lipid matrix. The DLS study was used to characterize the particle size. It confirmed the particle size distribution in the nanoparticulate region of 111.78 nm and a PDI of 24% indicated the monodisperse nature of the particles. The mean zeta potential of -26.3 ± 1.3 mV indicated good stability of the SLNs. Moreover, the SLNs having a z-average of 111.78 nm and PDI of 24% showed good drug entrapment as well as a good drug-loading capacity. *In-vitro* release kinetics revealed a first-order release pattern following the Higuchi model, showing a slow, linear and constant release of 48 h, indicating the potential of the formulated SLNs for prolonged release. Moreover, the release of β-carotene from the SLNs followed a diffusion-type release mechanism. The nanoparticles also demonstrated significant physical stability over six months. Finally, the anti-cancer activity of β-carotene-loaded SLNs was compared with the intact β-carotene on the MCF7 human BC cell line by MTT assay. The anti-cancer activity of SLNs was superior compared to pure β-carotene. In conclusion, the results of the current study show that β-carotene SLNs have long-term anticancer activity compared with intact β-carotene. In addition, related *in-vivo* studies in animal models may help to substantiate the improved cytotoxicity and pharmacokinetics of β-carotene SLNs.

Data availability statement

Currently, the raw data cannot be made available online as the data is also part of an ongoing study. However, this data can be made available to readers on request at rajatsubhra7@gmail.com.

CRediT authorship contribution statement

Rajat Subhra Dutta: Supervision, Data curation, Conceptualization. **Gamal Osman Elhassan:** Validation, Formal analysis. **Takhellambam Bidyapati Devi:** Writing – review & editing, Writing – original draft. **Bedanta Bhattacharjee:** Writing – review & editing, Writing – original draft. **Mohini Singh:** Writing – review & editing, Writing – original draft. **Bani Kumar Jana:** Writing – review & editing. **Supriya Sahu:** Investigation, Formal analysis. **Bhaskar Mazumder:** Writing – review & editing, Writing – original draft. **Ram Kumar Sahu:** Writing – review & editing, Writing – original draft. **Jiyauddin Khan:** Writing – review & editing.

Declaration of competing interest

The authors declare the following financial interests/personal relationships which may be considered as potential competing interests: We have no conflict of interest If there are other authors, they declare that they have no known competing financial interests or personal relationships that could have appeared to influence the work reported in this paper.

Acknowledgments

The researchers would like to thank the Deanship of Scientific Research, Qassim University for funding the publication of this manuscript.

References

[1] V.P. Chavda, S. Vuppu, R. Bezbaruah, L.V. Nalla, S.N.R. Gajula, P.C. Balar, T. Mishra, N. Sharma, S. Kamaraj, T. Suresh, Phytochemical loaded nanovehicles of biopolymer for breast cancer: a systemic review, Clinical Complementary Medicine and Pharmacology (2023) 100114.
[2] C. Rossi, I. Cicalini, M.C. Cufaro, A. Consalvo, P. Upadhyaya, G. Sala, I. Antonucci, P. Del Boccio, L. Stuppia, V. De Laurenzi, Breast cancer in the era of integrating "Omics" approaches, Oncogenesis 11 (1) (2022) 17.
[3] S. Łukasiewicz, M. Czeczelewski, A. Forma, J. Baj, R. Sitarz, A. Stanisławek, Breast cancer—epidemiology, risk factors, classification, prognostic markers, and current treatment strategies—an updated review, Cancers 13 (17) (2021) 4287.
[4] A.N. Giaquinto, H. Sung, K.D. Miller, J.L. Kramer, L.A. Newman, A. Minihan, A. Jemal, R.L. Siegel, Breast cancer statistics, 2022,, CA: a cancer journal for clinicians 72 (6) (2022) 524–541.
[5] M. Arnold, E. Morgan, H. Rumgay, A. Mafra, D. Singh, M. Laversanne, J. Vignat, J.R. Gralow, F. Cardoso, S. Siesling, Current and future burden of breast cancer: global statistics for 2020 and 2040, Breast 66 (2022) 15–23.
[6] L. Lin, S. Baritaki, S. Vivarelli, L. Falzone, A. Scalisi, M. Libra, B. Bonavida, The breast cancer protooncogenes HER2, BRCA1 and BRCA2 and their regulation by the iNOS/NOS2 Axis, Antioxidants 11 (6) (2022) 1195.
[7] Y. Herdiana, P. Husni, S. Nurhasanah, S. Shamsuddin, N. Wathoni, Chitosan-based nano systems for natural antioxidants in breast cancer therapy, Polymers 15 (13) (2023) 2953.
[8] B. Smolarz, A.Z. Nowak, H. Romanowicz, Breast cancer-epidemiology, classification, pathogenesis and treatment (review of literature), Cancers 14 (10) (2022) 2569.
[9] R.E. Nicoletto, C.M. Ofner III, Cytotoxic mechanisms of doxorubicin at clinically relevant concentrations in breast cancer cells, Cancer Chemother. Pharmacol. 89 (3) (2022) 285–311.
[10] A. Moammeri, K. Abbaspour, A. Zafarian, E. Jamshidifar, H. Motasadizadeh, F. Dabbagh Moghaddam, Z. Salehi, P. Makvandi, R. Dinarvand, pH-responsive, adorned nanoniosomes for codelivery of cisplatin and epirubicin: synergistic treatment of breast cancer, ACS Appl. Bio Mater. 5 (2) (2022) 675–690.
[11] S.K. Dubey, T. Bhatt, M. Agrawal, R.N. Saha, S. Saraf, A. Alexander, Application of chitosan modified nanocarriers in breast cancer, Int. J. Biol. Macromol. 194 (2022) 521–538.
[12] Z. Wang, X. Yang, J. Wang, S. Wang, X. Mao, M. Li, Y. Zhao, W. Wang, X. Qi, T. Wu, Risk of serious adverse event and fatal adverse event with molecular target anticancer drugs in cancer patients: a meta-analysis, J. Cancer Res. Therapeut. 15 (7) (2019) 1435–1449.
[13] M.R. Islam, F. Islam, M.H. Nafady, M. Akter, S. Mitra, R. Das, H. Urmee, S. Shohag, A. Akter, K. Chidambaram, Natural small molecules in breast cancer treatment: understandings from a therapeutic viewpoint, Molecules 27 (7) (2022) 2165.
[14] I. Peraita-Costa, P. Carrillo Garcia, M. Morales-Suarez-Varela, Is there an association between β-carotene and breast cancer? A systematic review on breast cancer risk, Nutr. Cancer 74 (1) (2022) 39–54.
[15] H. Rostamabadi, S.R. Falsafi, S.M. Jafari, Nanoencapsulation of carotenoids within lipid-based nanocarriers, J. Contr. Release 298 (2019) 38–67.
[16] J. Yu, Q. Mu, M. Fung, X. Xu, L. Zhu, R.J. Ho, Challenges and opportunities in metastatic breast cancer treatments: nano-drug combinations delivered preferentially to metastatic cells may enhance therapeutic response, Pharmacol. Ther. 236 (2022) 108108.
[17] M.K. Dehnavi, S. Ebrahimpour-Koujan, K. Lotfi, L. Azadbakht, The association between circulating carotenoids and risk of breast cancer: a systematic review and dose–response meta-analysis of prospective studies, Adv. Nutr. 15 (1) (2024) 100135.
[18] R. Pandiselvam, S. Mitharwal, P. Rani, M.A. Shanker, A. Kumar, R. Aslam, Y.T. Barut, A. Kothakota, S. Rustagi, D. Bhati, The influence of non-thermal technologies on color pigments of food materials: an updatedreview, Curr. Res. Food Sci. (2023) 100529.
[19] G.R. Mahrous, N.S. Elkholy, G. Safwat, M.W. Shafaa, Enhanced cytotoxic activity of beta carotene conjugated liposomes towards breast cancer cell line: comparative studies with cyclophosphamide, Anti Cancer Drugs 33 (1) (2022) e462–e476.
[20] N. Boonlao, U.R. Ruktanonchai, A.K. Anal, Enhancing bioaccessibility and bioavailability of carotenoids using emulsion-based delivery systems, Colloids Surf. B Biointerfaces 209 (2022) 112211.
[21] M.R. Shishir, L. Xie, C. Sun, X. Zheng, W. Chen, Advances in micro and nano-encapsulation of bioactive compounds using biopolymer and lipid-based transporters, Trends Food Sci. Technol. 78 (2018) 34–60.
[22] C. Soukoulis, T. Bohn, A comprehensive overview on the micro-and nano-technological encapsulation advances for enhancing the chemical stability and bioavailability of carotenoids, Crit. Rev. Food Sci. Nutr. 58 (1) (2018) 1–36.
[23] P.P. Dos Santos, L.d.A. Andrade, S.H. Flôres, A.d.O. Rios, Nanoencapsulation of carotenoids: a focus on different delivery systems and evaluation parameters, J. Food Sci. Technol. 55 (2018) 3851–3860.
[24] R. Ferrari, M. Sponchioni, M. Morbidelli, D. Moscatelli, Polymer nanoparticles for the intravenous delivery of anticancer drugs: the checkpoints on the road from the synthesis to clinical translation, Nanoscale 10 (48) (2018) 22701–22719.
[25] K. Trofymchuk, J. Valanciunaite, B. Andreiuk, A. Reisch, M. Collot, A.S. Klymchenko, BODIPY-loaded polymer nanoparticles: chemical structure of cargo defines leakage from nanocarrier in living cells, J. Mater. Chem. B 7 (34) (2019) 5199–5210.
[26] A. Rehman, Q. Tong, S.M. Jafari, E. Assadpour, Q. Shehzad, R.M. Aadil, M.W. Iqbal, M.M. Rashed, B.S. Mushtaq, W. Ashraf, Carotenoid-loaded nanocarriers: a comprehensive review, Adv. Colloid Interface Sci. 275 (2020) 102048.
[27] L.S. Schwartzberg, R.M. Navari, Safety of polysorbate 80 in the oncology setting, Adv. Ther. 35 (2018) 754–767.
[28] E. Russo, C. Villa, Poloxamer hydrogels for biomedical applications, Pharmaceutics 11 (12) (2019) 671.
[29] R.R. Vakhariya, V.R. Salunkhe, D.S. Randive, M.A. Bhutkar, S.D. Bhinge, Design, development and optimization of ramipril solid lipid nanoparticles using solvent emulsification and evaporation method, Nanosci. Nanotechnol. - Asia 11 (1) (2021) 42–52.
[30] P. Mura, F. Maestrelli, M. D'Ambrosio, C. Luceri, M. Cirri, Evaluation and comparison of solid lipid nanoparticles (SLNs) and nanostructured lipid carriers (NLCs) as vectors to develop hydrochlorothiazide effective and safe pediatric oral liquid formulations, Pharmaceutics 13 (4) (2021) 437.
[31] P. Karnjanawipagul, W. Nittayanuntawech, P. Rojsanga, L. Suntornsuk, Analysis of β-carotene in carrot by spectrophotometry, Mahidol University Journal of Pharmaceutical Science 37 (8) (2010).
[32] A. Akhoond Zardini, M. Mohebbi, R. Farhoosh, S. Bolurian, Production and characterization of nanostructured lipid carriers and solid lipid nanoparticles containing lycopene for food fortification, J. Food Sci. Technol. 55 (1) (2018) 287–298.
[33] R. Osanlou, M. Emtyazjoo, A. Banaei, M.A. Hesarinejad, F. Ashrafi, Preparation of solid lipid nanoparticles and nanostructured lipid carriers containing zeaxanthin and evaluation of physicochemical properties, Colloids Surf. A Physicochem. Eng. Asp. 641 (2022) 128588.

[34] S.G. Laime, C.C. Hernández, A.M. García, J.A. Payrol, Application of nanoformulations in improving the properties of curcuma (curcuma longa L.), in: Application of Nanotechnology in Food Science, Processing and Packaging, Springer, 2022, pp. 203–219.
[35] E. Nazemiyeh, M. Eskandani, H. Sheikhloie, H. Nazemiyeh, Formulation and physicochemical characterization of lycopene-loaded solid lipid nanoparticles, Adv. Pharmaceut. Bull. 6 (2) (2016) 235.
[36] M.D. Triplett, J.F. Rathman, Optimization of β-carotene loaded solid lipid nanoparticles preparation using a high shear homogenization technique, J. Nanoparticle Res. 11 (2009) 601–614.
[37] P. Jayachandran, S. Ilango, V. Suseela, R. Nirmaladevi, M.R. Shaik, M. Khan, M. Khan, B. Shaik, Green synthesized silver nanoparticle-loaded liposome-based nanoarchitectonics for cancer management: in vitro drug release analysis, Biomedicines 11 (1) (2023) 217.
[38] M.A. Siraj, A.T. Jacobs, G.T. Tan, B. Altersolanol, A fungal tetrahydroanthraquinone, inhibits the proliferation of estrogen receptor-expressing (ER+) human breast adenocarcinoma by modulating PI3K/AKT, p38/ERK MAPK and associated signaling pathways, Chem. Biol. Interact. 359 (2022) 109916.
[39] M. Dawoud, M. Mojally, R. Abdou, H.G. Attia, Comparative study on the performance of monoolein cubic nanoparticles and trimyristin solid lipid nanoparticles as carriers for docetaxel, Pharmaceut. Dev. Technol. 28 (3–4) (2023) 277–287.
[40] A. Hejri, A. Khosravi, K. Gharanjig, M. Hejazi, Optimisation of the formulation of β-carotene loaded nanostructured lipid carriers prepared by solvent diffusion method, Food Chem. 141 (1) (2013) 117–123.
[41] R.H. Myers, D.C. Montgomery, C.M. Anderson-Cook, Response Surface Methodology: Process and Product Optimization Using Designed Experiments, John Wiley & Sons, 2016.
[42] T. Mehmood, A. Ahmad, A. Ahmed, Z. Ahmed, Optimization of olive oil based O/W nanoemulsions prepared through ultrasonic homogenization: a response surface methodology approach, Food Chem. 229 (2017) 790–796.
[43] M. Schubert, C. Müller-Goymann, Solvent injection as a new approach for manufacturing lipid nanoparticles–evaluation of the method and process parameters, Eur. J. Pharm. Biopharm. 55 (1) (2003) 125–131.
[44] J. Zhang, Y. Fan, E. Smith, Experimental design for the optimization of lipid nanoparticles, J. Pharmaceut. Sci. 98 (5) (2009) 1813–1819.
[45] A.A. Adem, A. Belete, K.K. Lai, C. Hage, R.H. Neubert, T. Gebre-Mariam, Nanoemulgel formulation for topical delivery of plant glucosylceramide: characterization and optimization, J. Drug Deliv. Sci. Technol. 79 (2023) 104056.
[46] Y. Weerapol, S. Manmuan, N. Chaothanaphat, S. Limmatvapirat, J. Sirirak, P. Tamdee, S. Tubtimsri, New approach for preparing solid lipid nanoparticles with volatile oil-loaded quercetin using the phase-inversion temperature method, Pharmaceutics 14 (10) (2022) 1984.
[47] V. Polychniatou, C. Tzia, Evaluation of surface-active and antioxidant effect of olive oil endogenous compounds on the stabilization of water-in-olive-oil nanoemulsions, Food Chem. 240 (2018) 1146–1153.